Solid Earth Discuss., 7, 3179–3197, 2015
www.solid-earth-discuss.net/7/3179/2015/
doi:10.5194/sed-7-3179-2015
© Author(s) 2015. CC Attribution 3.0 License.

Solid Earth Discussions
Open Access

This discussion paper is/has been under review for the journal Solid Earth (SE).
Please refer to the corresponding final paper in SE if available.

Analysis of crustal deformation and strain characteristics in the Tianshan Mountains with least-squares collocation

S. P. Li[1], G. Chen[1,2], and J. W. Li[1]

[1]Faculty of Information Engineering, China University of Geosciences, Wuhan 430074, China
[2]National Engineering Research Center for Geographic Information System, Wuhan 430074, China

Received: 13 October 2015 – Accepted: 18 October 2015 – Published: 9 November 2015

Correspondence to: G. Chen (ddwhcg@cug.edu.cn)

Published by Copernicus Publications on behalf of the European Geosciences Union.

Abstract

By fitting the observed velocity field of the Tianshan Mountains from 1992 to 2006 with least-squares collocation, we established a velocity field model in this region. The velocity field model reflects the crustal deformation characteristics of the Tianshan reasonably well. From the Tarim Basin to the Junggar Basin and Kazakh platform, the crustal deformation decreases gradually. Divided at 82° E, the convergence rates in the west are obviously higher than those in the east. We also calculated the parameter values for crustal strain in the Tianshan Mountains. The results for maximum shear strain exhibited a concentration of significantly high values at Wuqia and its western regions, and the values reached a maxima of $4.4 \times 10^{-8}\,\mathrm{a}^{-1}$. According to isogram distributions for the surface expansion rate, we found evidence that the Tianshan Mountains have been suffering from strong lateral extrusion by the basin on both sides. Combining this analysis with existing results for focal mechanism solutions from 1976 to 2014, we conclude that it should be easy for a concentration of earthquake events to occur in regions where maximum shear strains accumulate or mutate. For the Tianshan Mountains, the possibility of strong earthquakes in Wuqia–Jiashi and Lake Issyk-Kul will persist over the long term.

1 Introduction

The Tianshan Mountains represent a typical resurgent orogenic belt in the inland regions of the Eurasian block, and this area has continued to experience uplift since the early Cenozoic. Tectonic movement in these regions is rather strong, and this area is considered to be a seismically active zone. In the domestic Tianshan regions, many earthquakes such as the Manas earthquake in 1907 (Zhang et al., 1994), the Wuqia M_s 7.1 earthquake in 1985 (Feng, 1999), the Bachu–Jiashi M_s 6.8 earthquake in 2003 (Xu et al., 2006; Li et al., 2012), and the Wuqia M_s 6.7 earthquake in 2008 (Qiao et al., 2014) have happened. Most earthquakes here are caused by the convergence of re-

SED

7, 3179–3197, 2015

gional fault stresses. When the accumulation of stress has exceeded the shear strength of rocks, the rocks rupture and the instability subsides, which leads to the occurrence of earthquakes (Jiang et al., 2003). Studies of the characteristics of stress and strain in the Tianshan region are of great significance to the field of seismology because of the similarities between this region and other seismically active areas around the world.

The strain characteristics of the Tianshan Mountains have been analyzed with Global Positioning System (GPS) data in several studies, and most of this research has focused on the regions located in Wuqia–Jiashi, which lies in the southwestern territory (Wang et al., 2000; Zhang et al., 2004; Li et al., 2012). According to this research, the stress direction in these regions is nearly north–south and the maximal shear strain is relatively high, which indicates that these regions are dangerous zones where earthquakes will probably happen. Wang et al. (2007) calculated and obtained the distribution of strain in Tianshan and its adjacent regions by using GPS data from 1998 to 2004. Those results demonstrate that the direction of the main strain is nearly orthogonal to the strike of the Tianshan Mountains on the whole and the highest values of maximal shear strain are mainly concentrated in the vicinity of Lake Issyk-Kul and Jiashi.

In this paper, we estimated the strain parameters in Tianshan and its adjacent regions based on velocity results from 1992 to 2006 by using the least-square collocation method. We also analyzed the strain characteristics in these regions. Combined with location data for earthquake sources, we then discussed the relationship between the distributions of strains and seismic foci. Based on this discussion, many valuable conclusions were obtained.

SED
7, 3179–3197, 2015

2 Method

2.1 Least-squares collocation

Least-squares collocation is also known as collocation, and it is a technique that is mainly used for studying the Earth's gravity field; collocation was first proposed in the 1960s (Zou, 2003). The core idea of least-squares collocation is to consider both the influences of trend effects and random effects so that unified error equations can be established. Moreover, the random effects can be either from measured signals or estimated signals. As long as there are correlations between these signals, it is possible to use the measured signals to estimate other signals (Jiang and Liu, 2010). According to the theory of parameter adjustment or matrix inversion, the most probable value of trend and random signals can be obtained (Wu et al., 2009). The basic model of least-squares collocation is specified by

$$\boldsymbol{V} = \mathbf{A}\Omega + \mathbf{B}\boldsymbol{V}_\mathrm{s} + \boldsymbol{\varepsilon} \tag{1}$$

where $\boldsymbol{V}$ represents the observation vector for the points, $\mathbf{A}$ represents the coefficient matrices for the trend parameter Ω and observations, $\mathbf{B}$ (corresponding to the observed points, the matrix $\mathbf{B}$ is an identity) represents the coefficient matrix for the random signals $\boldsymbol{V}_\mathrm{s}$, and it reflects the contributions to the observation vector made by the random signals, and $\boldsymbol{\varepsilon}$ denotes the measurement noise vector. In addition, the optimum solutions for fixed parameter Ω and the random signals $\boldsymbol{V}_\mathrm{s}$ can be specified by

$$\hat{\Omega} = \{\mathbf{A}^T(\mathbf{C}_\mathrm{oo} + \mathbf{C}_\mathrm{nn})^{-1}\mathbf{A}\}^{-1}\mathbf{A}^T(\mathbf{C}_\mathrm{oo} + \mathbf{C}_\mathrm{nn})^{-1}\boldsymbol{V} \tag{2}$$

$$\hat{\boldsymbol{V}}_\mathrm{s} = \mathbf{C}_\mathrm{uo}(\mathbf{C}_\mathrm{oo} + \mathbf{C}_\mathrm{nn})^{-1}(\boldsymbol{V} - \mathbf{A}\hat{\Omega}) \tag{3}$$

where $\mathbf{C}_\mathrm{uo}$ represents the covariance matrix for the observed points and estimated point signals, $\mathbf{C}_\mathrm{oo}$ denotes the covariance matrix for the observed point signals, and $\mathbf{C}_\mathrm{nn}$ is the covariance matrix for observation errors.

SED
7, 3179–3197, 2015

CC BY

When we build the regional strain field by using the GPS velocity field, we can treat the Euler vectors as trend parameters and take the relative movement between the observation points, in which the rigid rotation part has been subtracted, as the random signals. When estimating the parameters $\hat{\Omega}$ and $\hat{\boldsymbol{V}}_s$, we only know $\mathbf{C}_{nn}$ in the three covariance matrices, while the matrices $\mathbf{C}_{uo}$ and $\mathbf{C}_{oo}$ are unknown. Previous studies have shown that the local covariance distributions of crustal deformation observation signals are generally in accord with the Gaussian covariance distribution (Yoichiro, 1994). Therefore, in this paper, we used the Gaussian empirical covariance function to structure the covariance matrices $\mathbf{C}_{uo}$ and $\mathbf{C}_{oo}$ the function can be specified by

$$f(d) = f(0)\exp(-k^2 d^2) \tag{4}$$

where d denotes the distance between the signals, $f(0)$ represents the initial covariance, and k is the parameter to be determined. With increments of distance between signal points, the covariance reduces gradually until it converges to zero, which corresponds with the basic requirements for weighting criteria in adjustment theory. $f(0)$ can be calculated according to Eq. (5) (Zhang and Jiang, 1999):

$$f(0) = f_v(0) - f_\varepsilon(0) \tag{5}$$

where $f_v(0)$ usually is represented by the average sum of squares of observations and $f_\varepsilon(0)$ takes the average sum of squares of the observations' root mean square error.

2.2 Calculation of strain parameters

A crucial step when building the regional strain field by using the velocity field is to express the velocity field of the study area as a function of geographical coordinates. In this way, we can calculate the corresponding strain parameters by using the partial derivative relations between deformation and strain. If we want to solve the strain field in the sphere surface, the geographic coordinates are the corresponding latitude and longitude (λ, φ). If it is in the Gauss plane, the corresponding Gauss plane coordinates

CC BY

(X, Y) should be used. By analyzing the differences between the strain parameters calculated separately by using the sphere surface and Gaussian plane coordinate system, Shi and Zhu (2006) proposed that we should use spherical coordinates when calculating strain parameters. However, considering the fact that the span of our research region in this paper is moderate and the differences in the results between the spherical coordinate system and Gauss plane coordinate system are not significant, we still used the Gauss plane coordinate system to calculate the strain parameters. Supposing that the velocity of one point (x, y) on the Gauss plane is (u, v), the strain parameter can be specified by

$$\varepsilon_x = \frac{\partial_u}{\partial_x}, \quad \varepsilon_y = \frac{\partial_v}{\partial_y}, \quad \varepsilon_{xy} = \frac{1}{2}\left(\frac{\partial_u}{\partial_x} + \frac{\partial_v}{\partial_y}\right) \tag{6}$$

where ε_x and ε_y represent the linear strain in the separate x and y directions, respectively, and ε_{xy} denotes the shear strain.

The maximum and minimum principal strain, maximum shear strain, and surface expansion (Jin and Park, 2007; Jiang et al., 2008) can be specified, respectively, by

$$\varepsilon_1 = \frac{\varepsilon_x + \varepsilon_y}{2} + \sqrt{((\varepsilon_x - \varepsilon_y)/2)^2 + \varepsilon_{xy}^2} \tag{7}$$

$$\varepsilon_2 = \frac{\varepsilon_x + \varepsilon_y}{2} - \sqrt{((\varepsilon_x - \varepsilon_y)/2)^2 + \varepsilon_{xy}^2} \tag{8}$$

$$\gamma_{\max} = \frac{1}{2}(\varepsilon_1 - \varepsilon_2) \tag{9}$$

$$\Delta = \varepsilon_1 + \varepsilon_2 \tag{10}$$

2.3 Estimation of the strain field in the Tianshan Mountains

Yang et al. (2008) processed GPS data for the Tianshan Mountains and the adjacent regions from 1992 to 2006 by using GIPSY software and the time series analysis

CC BY

method. After that, the GPS velocity field including 368 local stations relative to the stable Eurasian block was obtained (Fig. 1). The statistical result for the velocity precision showed that the horizontal precision for most stations is better than $2\,\mathrm{mm\,a^{-1}}$. Therefore, we can use the least-squares collocation technique to estimate the distribution of the strain parameters in this region by using Yang's velocity field as input data.

First, we calculated the Euler vector for the entire area by using least-squares collocation. Then, we took the relative movement between the observation points, in which the rigid rotation part had been subtracted, as the random signals. In the range of 72–95° E longitude and 35–47° N latitude, we obtained 1175 estimated signal points by splitting the area uniformly according to a uniform grid of 0.5°. The empirical function proposed by Zhang and Jiang (1999) was used to determine the optimal value of parameter K in the covariance function:

$$K_{\min} = \sqrt{\frac{-\ln(10^{-3})}{S^2}} \tag{11}$$

where S represents the relevant range of the entire area. Experience shows that the relevant range S is generally between one-fourth to one-half of the maximal distance (Zhang and Jiang, 1999). In this paper, the maximal distance was 1815.5 km, so the value of parameter K was taken to be between 0.0029–0.0058 according to the Eq. (11). We chose a value of K equal to 0.0037 when the Gauss empirical covariance function (Fig. 2) provided a good fit to the covariance of random signals. Figure 2 shows that the relevant range of signal points was about 600 km. When outside of this range, the correlation coefficient converged to zero. Then, we were able to use the Gaussian covariance function to construct covariance matrices $\mathbf{C}_{\mathrm{uo}}$ and $\mathbf{C}_{\mathrm{oo}}$. After we calculated the covariance matrix of estimated points, we obtained the velocity vector of the 1175 estimated points (Fig. 3).

SED
7, 3179–3197, 2015

3 Results and discussion

3.1 Crustal deformation characteristics in the Tianshan Mountains

From an overall perspective, the estimated velocities agreed well with the observed velocity vectors of stations in terms of both values and directions. However, at a small number of stations, for example, CHG4, I029, and I059, inconsistencies between modeled velocities and observed velocities were detected. We conjecture that this kind of anomaly is mainly due to the local deformation that is caused by non-uniform tectonic movement of local faults near the stations. The variation of the estimated velocity field reflects the crustal deformation characteristics of the Tianshan Mountains as a whole. From the Tarim Basin to the Junggar Basin and Kazakh platform, the crustal deformation decreases in a gradual manner, which generates the crustal convergence deformation. In the Tianshan Mountains, the distribution of convergence deformation does not appear in a linear and uniform way. Divided at 82° E, the convergence rates in the west are higher than those in the east (Niu et al., 2007; Wang et al., 2007). During the transition from the area east of Pamirs to the area west of the Tarim Basin, the directions of simulative vectors change from NNW to N. This indicates that a divergent component exists in the interior of the Pamir relative to the Tarim Basin, despite of the presence of thrust faults along their boundary, which is consistent with the conclusions obtained by the velocity profile method of Zubovich et al. (2010). In the west of Tarim Basin, the direction of velocity is north, however, in the east of the basin, the direction changes to NNE. It shows that Tarim basin may rotate clockwise around a pole. We calculated the rotation rate is about $0.314^\circ\,\mathrm{Ma}^{-1}$. Compared with the rotation rates of $0.65^\circ\,\mathrm{Ma}^{-1}$ estimated from geologic models (Wang et al., 2000) and $0.5203^\circ\,\mathrm{Ma}^{-1}$ from the work of Yang et al. (2008), our result is much smaller. The reason for these differences remains to be elucidated.

SED
7, 3179–3197, 2015

3.2 Crustal strain characteristics in the Tianshan Mountains

The result for the maximal shear strain in the Tianshan Mountains indicates that there are two concentration regions. One is located in the vicinity of Wuqia in the southwestern Tianshan, and the other is located at Lake Issyk-Kul in the northern Tianshan. Both of these concentration regions are located in strong crust shortening regions (Wang et al., 2000). This indicates that these regions have accumulated high amounts of shear strain due to the strong crustal uplift deformation since the early Cenozoic. The highest value of maximal shear strain reached $4.4 \times 10^{-8}\,\mathrm{a}^{-1}$ at a point located to the west of Wuqia County. While our numerical solutions are very close to the results given by Wang et al. (2000) and Zhang et al. (2004), they are quite different from the results obtained by Wang et al. (2007) and Li et al. (2012). Among the factors that may have contributed to the divergences, differences in the models and data sources cannot be ignored. The maximal shear strain in the vicinity of Lake Issyk-Kul was found to be $3 \sim 4 \times 10^{-8}\,\mathrm{a}^{-1}$, which is exceeded only by the region to the west of Wuqia County. Since the early Pleistocene, there has been significant subsidence movement on the bottom of Lake Issyk-Kul that has lasted for almost 2 Ma, and this movement may be related to the small-scale mantle convection that exists between the lower crust and upper mantle of this region (Tychkov et al., 2008). The subsidence of crust makes the shear stress between rocks increase constantly, and thus, there is convergence of the shear strain. The focal mechanism solutions (Fig. 4) indicate that the rupture of earthquakes in Wuqia and its adjacent regions is mainly dominated by inverse and thrust faults. In addition, many strike-slip earthquakes are involved (Qiao et al., 2014), which demonstrates that the power source causing frequent earthquakes in these regions might come from the northward push of the Pamir arc structural belt. On the whole, a corresponding relationship was found between the location of earthquakes and the gradient of maximal shear strain. As shown in Fig. 4, most of the past earthquakes ($M_w \geq 5.0$) in the Tianshan Mountains and adjacent regions were concentrated in Wuqia, Lake Issyk-Kul, and the neighboring regions where the maximal

SED
7, 3179–3197, 2015

CC BY

shear strain decreases sharply. Especially in the Kashgar and Jiashi region, strong earthquakes ($M_s > 6.0$) occurred continuously in 1997–1998 (Shan et al., 2002). The velocity results (Fig. 1) demonstrate that the size and direction of crust movement in these regions have changed significantly and the imbalance of crust movement facilitates the accumulation of strain. Generally, when the accumulation has exceeded the shear strength of rocks, the rocks rupture and the instability subsides, which leads to the occurrence of earthquakes. It is very likely that the potential for strong earthquakes in these regions will persist over long periods of time. In addition, the maximal shear strains in other regions (e.g., Aksu, Bortala, Shihezi, Manas) of the northern Tianshan Mountains are also relatively high, and many strong earthquake events have been concentrated in these regions (Fig. 4). For example, the source of the Manas earthquake ($M_s = 7.7$) in 1906 was located in the active reverse fault-fold zones of the northern Tianshan Mountains (Zhang et al., 1994). The maximal shear strains in the Tarim Basin and Junggar Basin, which are located on both sides of the Tianshan Mountains, are lower. This indicates that the intensity of tectonic activity in these two blocks is weaker than that in the Tianshan orogenic belt, which has been proven by other geological and geophysical research (Guo et al., 2006). It should be noted that the maximal shear strains in the vicinity of the Kunlun Mountains (right-bottom corner of Fig. 4) are lower. However, seismic activity in this region is hyperactive; for example, a large earthquake ($M_s = 8.1$) struck the Kunlun Mountains in 2001 (Zhang et al., 2003). The most likely reason for the discrepant results is that there are no observation stations distributed in this region and this leads to distortion of analog values. Therefore, the calculated results in this region were not considered in further analyses.

The distribution of surface expansion rates in the Tianshan Mountains (Fig. 5) had similar characteristics to the distribution of maximal shear strains. Surface expansion rates can reflect the variation characteristics of the horizontal area when the upper crust is impacted by the regional stress field (Zhang et al., 2004). If the surface expansion rate is negative, the area is being squeezed. On the contrary, if the rate is positive, this means that the crust is in the expanded state. Overall, we found evidence

CC BY

that the Tianshan Mountains are suffering from lateral extrusion by the basin on both sides. Combined with the results for the main strains, we think that the main extrusion direction in the western Tianshan Mountains is nearly northwest, and in the eastern Tianshan Mountains, it changes to nearly north. Guo et al. (2006) reconstructed the *P* wave velocity structure of the crust and upper mantle across Tianshan by using a seismic tomography technique. Their results also demonstrate that the Tianshan crust is compressed strongly by the Tarim block and Junggar Basin, and their data matched well with the shear strain results in this paper. As mentioned above, the Tarim Basin rotates clockwise around a pole. At the same time, the results for the surface expansion are suggestive of the existence of an expansion component in the basin (Wang et al., 2007), and this component's characteristics extend to the area east of the Pamirs plateau, which matches well with our simulated velocity field (Fig. 3).

4 Conclusions

In this study, we estimated the velocity field in the Tianshan Mountains by using the least-square collocation technique. Both the observed velocity field and simulated velocity field showed consistent features, and the variation of the estimated velocity field data reflected the crustal deformation characteristics of the Tianshan region. From south to north, the crustal deformation decreases gradually, which presents a kind of "catching-up style" orogenic pattern. In the east–west direction, divided at 82° E, the convergence rates in the west were found to be higher than those in the east.

We calculated the strain parameters for the Tianshan Mountains and adjacent regions by using the estimated velocity field. Then, we took the maximal shear strain and surface expansion as an example and analyzed the strain characteristics in various Tianshan regions. The results indicate that the Tianshan crust is compressed strongly by the Tarim block and Junggar Basin, especially in the transition zone between the basin and mountains. By evaluating earthquake events, we demonstrated that there is a corresponding relationship between the location of earthquakes and the gradient of

Discussion Paper | Discussion Paper | Discussion Paper | Discussion Paper |

SED

7, 3179–3197, 2015

Analysis of strain characteristics in Tianshan Mountains

S. P. Li et al.

maximal shear strain. The regions where maximal shear strains converge and show sudden change are more likely to experience earthquake events.

However, it should be noted that the GPS velocity data used in this paper cannot response the crustal deformation characteristics for recent years as the limited of the GPS data time span (1992–2006). It is expected that more current data would be adopted to analyze the kinematic and geodynamic characteristics for the Tianshan Mountains.

Acknowledgements. This work was supported by the National Natural Science Foundation of China (NSFC) (No. 41274036). We express special thanks to Yang Shaomin for providing the velocity data filed in her paper. Most of the figures were generated by using Generic Mapping Tools (GMT) software.

References

Feng, X.: The intensity and causative tectonics of the 1985 Wuqia, Xinjiang, earthquake, Inland Earthquake, 13, 169–178, 1999.

Guo, B., Liu, Q., and J., C.: Seismic tomography of the crust and upper mantle structure underneath the Chinese Tianshan, Chinese J. Geophys.-Ch., 49, 1693–1700, 2006.

Jiang, W. P., Zhou, X. H., and Liu, J. N.: Present-day crustal movement and strain rate in the Qinghai Tibetan Plateau from GPS data, Acta Geo. et Cart. Sin., 37, 285–292, 2008.

Jiang, Z. and Liu, J.: The method in establishing strain field and velocity field of crustal movement using least squares collocation, Chinese J. Geophys.-Ch., 53, 1109–1117, 2010.

Jiang, Z., Ma, Z., and Niu, A.: Approaches and preliminary results of crustal movement researches based on the GPS in China, Earth Science Frontiers, 10, 71–79, 2003.

Jin, S. G. and Park, P.: Tectonic activities and deformation in South Korea constrained by GPS observations, Int. J. Geology, 2, 11–15, 2007.

Li, J., Liu, D., and Wang, Q.: Research on the characteristics of recent crustal movement of the south Tianshan area in Xinjiang through the strain field and the change rate of baseline, J. Seismol. Res., 35, 59–65, 2012.

Niu, Z., You, X., and Yang, S.: Analysis of contemporary crustal deformation characteristics with GPS data of Tianshan Mountain, J. Geodesy Geodyn., 27, 1–9, 2007.

CC BY

Qiao, X., Wang, Q., and Yang, S.: Study on the focal mechanism and deformation characteristics for the 2008 M_w 6.7 Wuqia earthquake, Xinjiang by InSAR, Chinese J. Geophys.-Ch., 57, 1805–1813, 2014.

Shan, X., He, Y., and Zhu, Y.: A preliminary analysis on rupture characteristics of Jiashi strong earthquake swarm, Chinese J. Geophys.-Ch., 45, 416–425, 2002.

Shi, Y. and Zhu, S.: Discussion on method of calculating strain with GPS displacement data, J. Geodesy Geodyn., 26, 1–8, 2006.

Tychkov, S. A., Kuchai, O. A., and Bushenkova, N. A.: Current crustal deformation in the northern Tien Shan: GPS and seismological data, Russ. Geol. Geophys., 49, 280–290, doi:10.1016/j.rgg.2007.05.006, 2008.

Wang, Q., Ding, G., and Qiao, X.: Research on present crustal deformation in the southern Tianshan(Jiashi), China by GPS geodesy, Acta Seismologica Sinica, 22, 263–270, 2000.

Wang, X., Li, J., and Alexander, Z.: Horizontal movement and strain characteristics in Tianshan and its adjacent region with GPS deformation data, Acta Seismologica Sinica, 29, 31–37, 2007.

Wu, Y., Jiang, Z., and Yang, G.: The application and method of GPS strain calculation in whole mode using least square collocation in sphere surface, Chinese J. Geophys.-Ch., 52, 1707–1714, 2009.

Xu, X., Zhang, X., and Ran, Y.: The preliminary study on seismo tectonics of the 2003 ad Bachu-Jiashi earthquake (M_s 6.8), southern Tian Shan, Seismology and Geology, 28, 161–178, 2006.

Yang, S., Li, J., and Wang, Q.: The deformation pattern and fault rate in the Tianshan Mountains inferred from GPS observations, Sci. China Ser. D, 51, 1064–1080, 2008.

Yoichiro, F.: Estimation of Continuous Distribution of Earth's Strain in the Kanto-Tokai District, Central Japan With the Aid of Least Square Prediction, An Advanced Lecture on Geodesy in China, China Seismological Bureau, Xi'an, China, 1994.

Zhang, P., Deng, Q., and Xu, X.: Blind thrust, folding earthquake and the 1906 manas earthquake, Xinjiang, Seismology and Geology, 16, 193–204, 1994.

Zhang, P., Deng, Q., and Zhang, G.: The strong seismic activity and active block in Chinese mainland, Sci. China Ser. D, 33, 12–20, 2003.

Zhang, X. and Jiang, Z.: Study on some questions of dynamic pictures of crustal deformation and strain fields obtained by the least square collocation, Crustal Deformation and Earthquake, 19, 32–39, 1999.

SED

7, 3179–3197, 2015

CC BY

Zhang, Y., Sun, H., and Wang, W.: Characteristics of horizontal deformation in Jiashi area, Xinjiang Uygur autonomous region, J. Seismol. Res., 27, 179–183, 2004.
Zou, X.: The Application of Least-Squares Collocation in Physical Geodesy, master thesis, Wuhan University, Wuhan, China, 2003.
Zubovich, A. V., Wang, X., Scherba, Y. G., and Schelochkov, G. G.: GPS velocity field for the Tien Shan and surrounding regions, Tectonics, 29, 1–23, doi:10.1029/2010TC002772, 2010.

SED
7, 3179–3197, 2015

CC BY

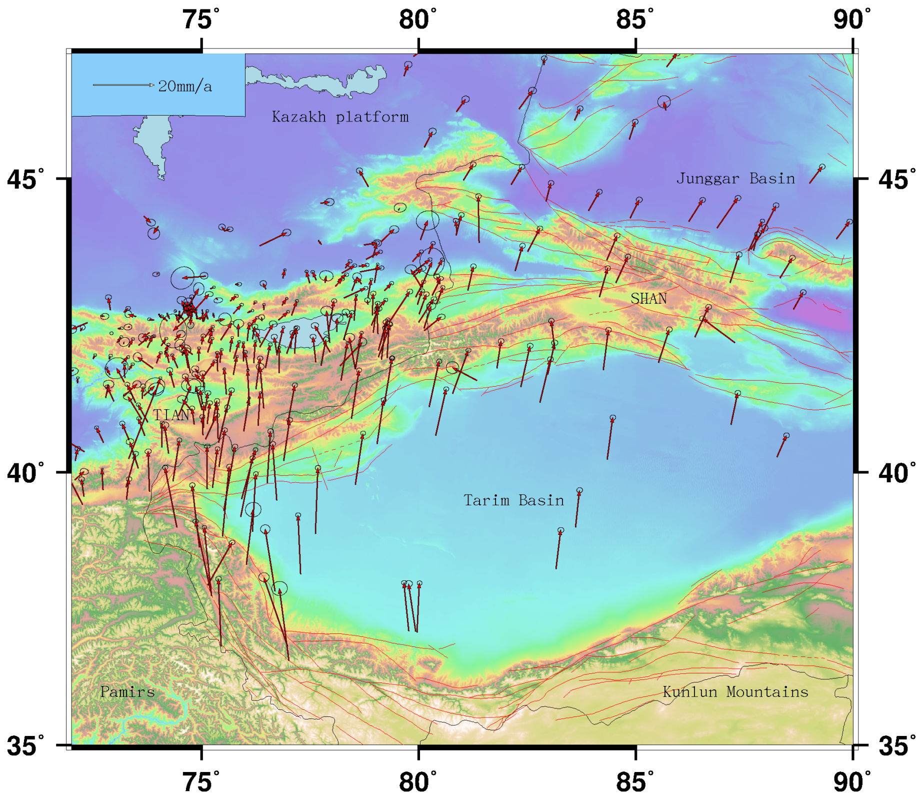

Figure 1. The velocity field for crustal horizontal movement from 1992 to 2006 in the Tianshan Mountains (arrows show the movement rate and its orientation to the error ellipse at a 95 % confidence level; red solid lines denote the distribution of faults).

SED
7, 3179–3197, 2015

Analysis of strain characteristics in Tianshan Mountains

S. P. Li et al.

cc BY

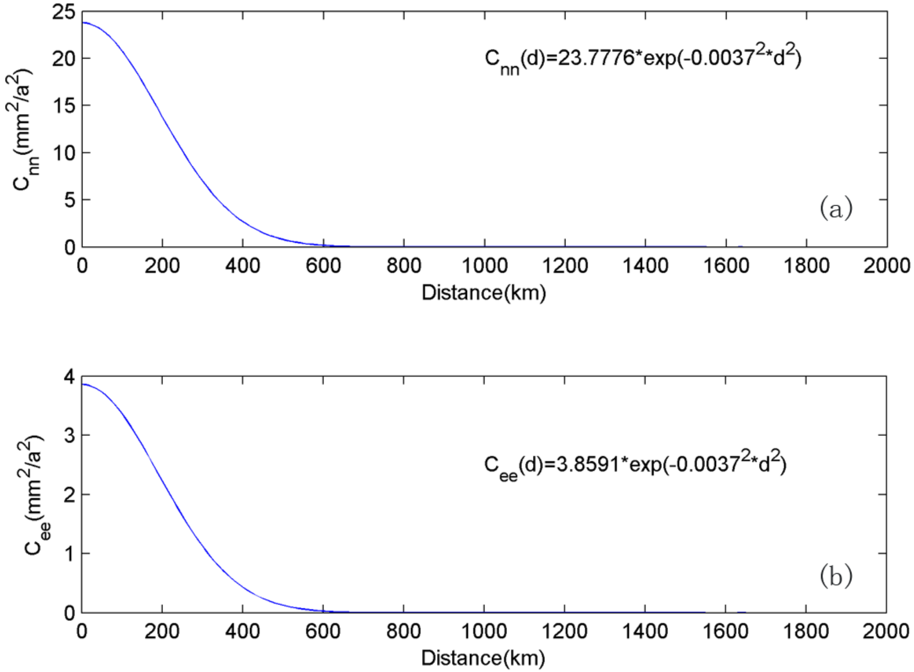

Figure 2. The Gaussian covariance functions in the north–south **(a)** and east–west **(b)** directions of the study area.

CC BY

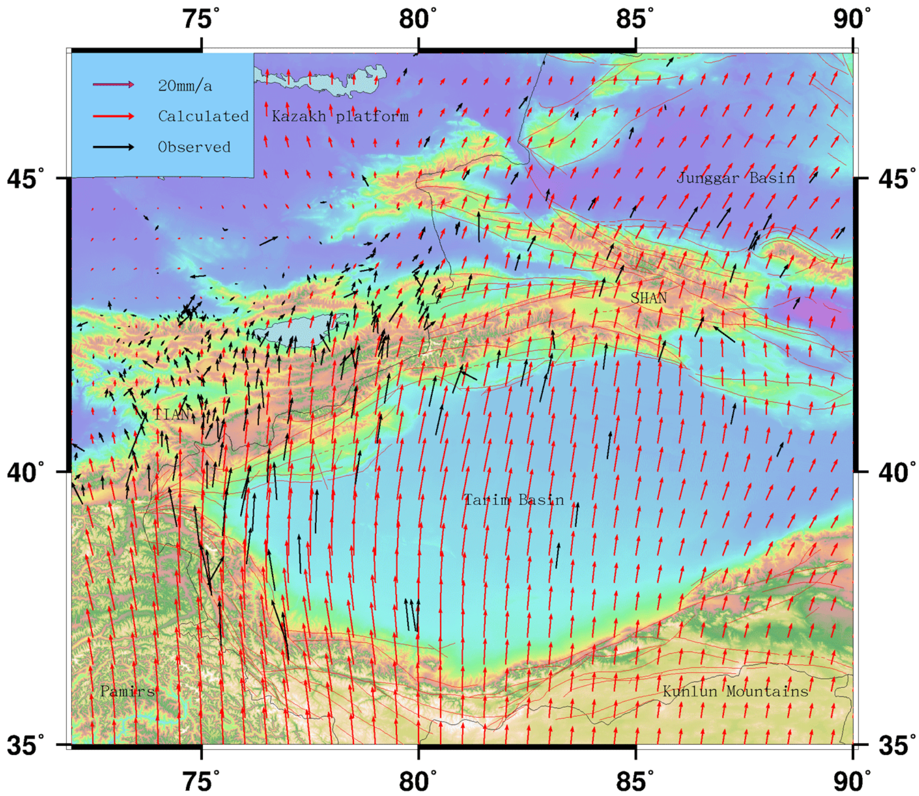

Figure 3. The velocity model for the Tianshan Mountains and its adjacent regions (red arrows represent the size and direction of the simulative velocity and block arrows denote the size and direction of the measured velocity; the size of the simulative grid is 0.5° × 0.5°).

SED
7, 3179–3197, 2015

CC BY

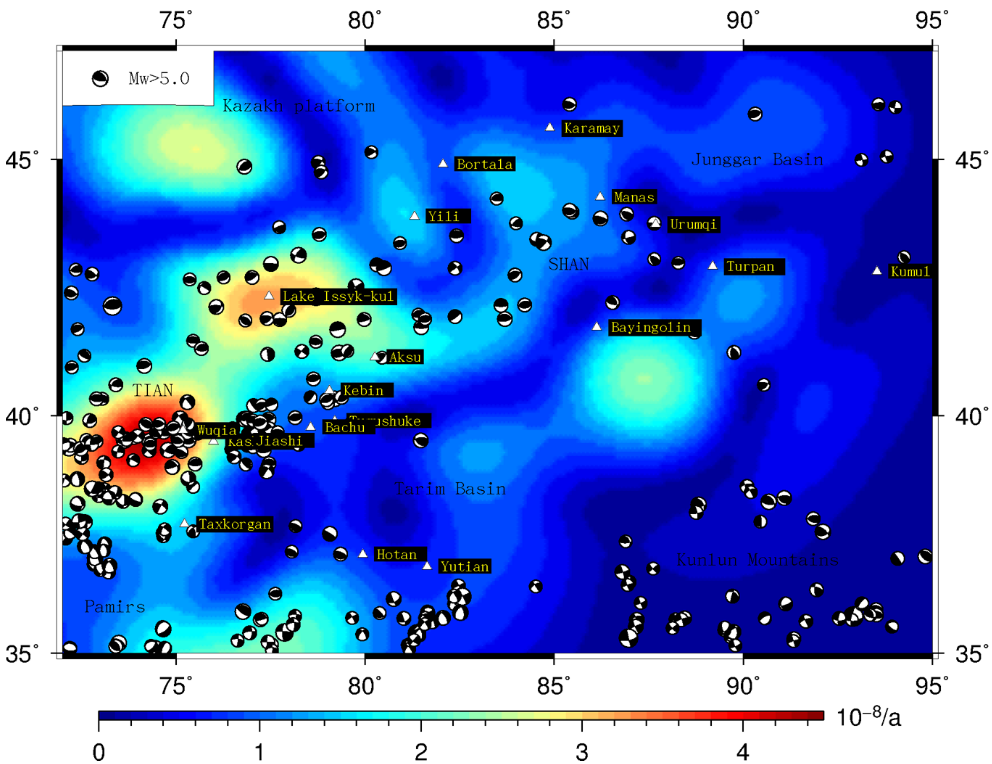

Figure 4. The isogram distributions of maximal shear strain in the Tianshan Mountains (the focal mechanism solution comes from the Global CMT (Centroid–Moment–Tensor) Project of Harvard University; the time span is from 1976 to 2014).

SED
7, 3179–3197, 2015

CC BY

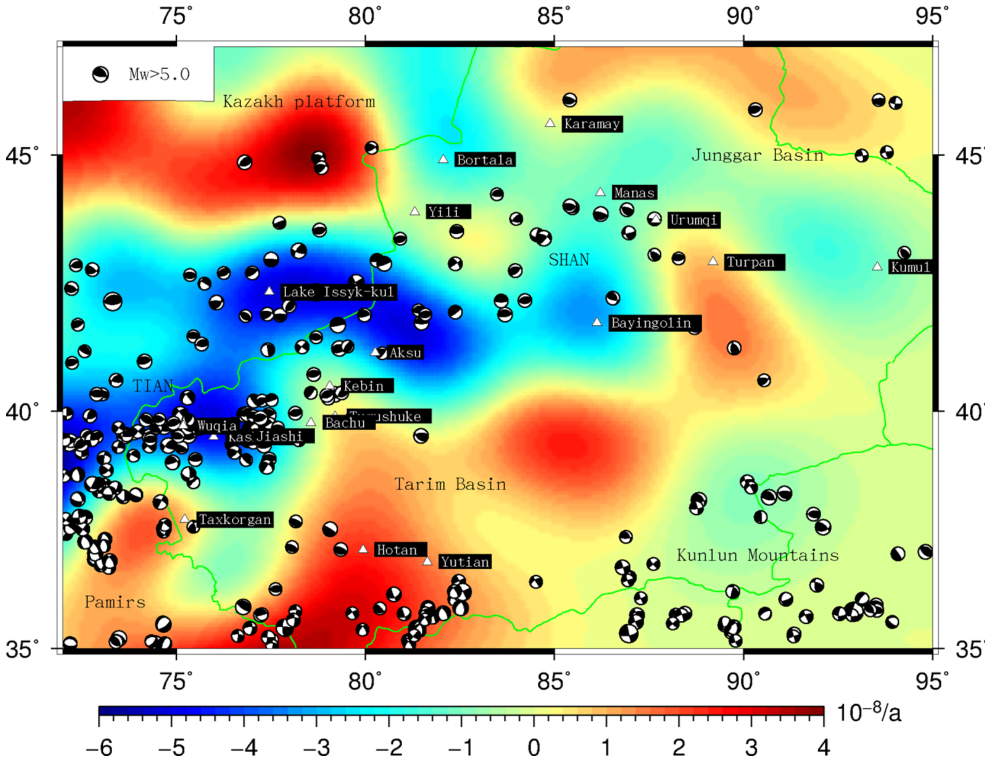

Figure 5. The isogram distributions for the surface expansion rate in the Tianshan Mountains.

SED
7, 3179–3197, 2015

Analysis of strain characteristics in Tianshan Mountains

S. P. Li et al.

Title Page
Abstract
Introduction
Conclusions
References
Tables
Figures
◀
▶
Back
Close
Full Screen / Esc
Printer-friendly Version
Interactive Discussion

CC BY